Controlling Silver Release from Antibacterial Surface Coatings on Stainless Steel for Biofouling Control

by

Kiarash Ranjbari

A Thesis Presented in Partial Fulfillment
of the Requirements for the Degree
Master of Science

Approved April 2021 by the
Graduate Supervisory Committee:

François Perreault, Chair
Morteza Abbaszadegan
Mohammed Rafiqul Islam

ARIZONA STATE UNIVERSITY

May 2021

ABSTRACT

Iodine and silver ions (Ag^+), added as silver fluoride (AgF) or silver nitrate ($AgNO_3$), are currently being used as a biocide to control the spread of bacteria in the water storage tanks of the International Space Station (ISS). Due to the complications of the iodine system, NASA is interested to completely replace iodine with silver and apply it as an antibacterial surface coating on stainless steel (SS) surfaces for biofouling control in extended space missions. However, Ag^+ is highly soluble and rapidly dissolves in water, as a result, the coated surface loses its antibacterial properties. The dissolution of NPs into Ag^+ and subsequent solubilization reduces its effectivity or extended period application. This study focuses on the *in-situ* nucleation of silver nanoparticles (AgNP) on stainless steel followed by their partial passivation by the formation of a low solubility silver sulfide (Ag_2S), silver bromide (AgBr), and silver iodide (AgI) shell with various concentrations for an increased long-term biofouling performance and a slower silver release over time. Antibacterial activity was evaluated using *Pseudomonas aeruginosa*. The highest bacterial inactivation (up to 75%) occurred with sulfidized AgNPs as opposed to bromidized (up to 50%) and iodized NPs (up to 60%). Surface analysis by scanning electron microscopy (SEM) showed considerably fewer particles on AgBr and AgI compared to Ag_2S-coated samples. Silver iodide was not tested in additional experiments due to its drawbacks and its poor antibacterial performance compared to sulfidized samples. Compared to pristine AgNPs, Ag release from both sulfidized and bromidized NPs was significantly low (16% vs 6% or less) depending on the extent of sulfidation or bromidation. Experiments were also carried out to investigate the effect of passivation on biofilm formation. Biofilm growth was

smaller on surfaces treated with 10^{-3} M Na_2S and 10^{-3} M NaBr compared to the surface of pristine AgNPs. Overall, sulfidation appears to be the most effective option to control biofilm formation on stainless steel. However, future research is needed to verify the effectiveness of sulfidized AgNPs on other metals including Inconel 718 and Titanium 6Al-4V used in the spacecraft potable water systems.

DEDICATION

I would like to dedicate this thesis to my family, especially to my mother, Leila. Mom, I would not be where I am today without you. Thank you for your endless love, support, advice, sacrifices, and for always being there for me through ups and downs. Nasim, there is no better sister than you. You are my best friend and my travel companion in all the adventures. Thank you for having my back and supporting me all the time. My world is brighter because of you.

ACKNOWLEDGMENTS

First and foremost, I would like to express my sincere gratitude to my committee chair and advisor Dr. Francois Perreault for his invaluable support from the very beginning when I joined his group. Francois, you have been a tremendous mentor for me. Thank you for all your guidance, for encouraging my research, and most importantly for sharing your knowledge and expertise with me throughout my entire graduate school career.

I would like to thank my professor, thesis committee member and mentor Dr. Morteza Abbaszadegan for guiding me both in a professional and a personal level over the past two years. I had the best memories of my master's degree in your microbiology class. I would also like to thank my other committee member and advisor, Dr. Rafiqul Islam for his sincere support, and for giving me the opportunity to work on exciting research projects.

Thank you to my lab mates and team members for all the good memories we have made so far while working in the lab together and outside of the school. I look forward to making more memories with you in the future.

I would like to acknowledge the School of Sustainable Engineering and the Built Environment at Arizona State University for all the opportunities it has given me to progress both as a student and as an engineer. Lastly, I thank the National Science Foundation's Center for Nanotechnology-Enabled Water Treatment (NEWT) for providing financial support, effective mentoring, and internships with industry partners.

TABLE OF CONTENTS

Page

LIST OF FIGURES

CHAPTER 1

INTRODUCTION

1.1 Motivation of this work

The development of a long-term strategy that can control the proliferation of microorganisms and prevent biofilm growth in drinking water systems of International Space Station (ISS) is among the major topics that have drawn considerable attention to it (Kim, Tengra, Young, et al., 2013; Zea et al., 2020). Currently, iodine or silver compounds such as fluoride (AgF) and silver nitrate ($AgNO_3$) are used as disinfectants in the potable water systems (PWS) of the ISS (Birmele et al., 2020; Williamson & Emmert, 2013). Although iodine has low human toxicity thresholds and it is an effective disinfectant, it also has various disadvantages in space missions. Iodine produces a poor taste, needs to be frequently replaced as it quickly loses its efficacy, and has high total organic carbon (TOC) which leads to disinfection by products DBPs. Therefore, NASA is considering to completely replace iodine with silver as an alternative antibacterial and anti-biofouling agent for extended spaceflight missions (Birmele et al., 2012, 2020; Roberts et al., 2007).

Silver is a known biocide used for disinfection in the potable water systems on the Russian side of the International Space Station (ISS) due to its capacity to inactivate pathogens without leaving toxic disinfection residues (Q. Li et al., 2008; Williamson & Emmert, 2013). Besides, silver is relatively safe for human consumption at a controlled concentration level and does not need to be filtered out of the water before consumption (Deshmukh et al., 2019; W. Li et al., 2018; Nowack et al., 2011; WHO, 2018). However, silver ions (Ag^+) have limitations when it comes to long term control of biofilm growth in water treatment systems. The water-soluble silver forms tend to quickly react with water

inside the water storage systems and are quickly removed from metallic surfaces over a short period of time (Birmele et al., 2020).

Silver nanoparticles (AgNPs) have been frequently used for biofouling control on a variety of surfaces for biomedical systems and water treatment (Q. Li et al., 2008; Marambio-Jones & Hoek, 2010; Rice et al., 2018; Sambhy et al., 2006; Silvestry-Rodriguez et al., 2008; Tylkowski et al., 2019). Their promising behavior is primarily due to their high specific surface area, which enhance dissolution into silver ions or increase contact-mediated antimicrobial effects when the bacteria come into contact with the surface (Alissawi et al., 2012; Verkhovskii et al., 2019; Zawadzka et al., 2014). The high solubility of silver is favorable in a biomedical setting since it allows for a quick bacterial inactivation (Burdușel et al., 2018). However, for long-term applications, silver ions immediately solubilize in water in the presence of oxygen, and the surface promptly loses its antimicrobial properties (Rahaman et al., 2014).

To reduce silver nanoparticle solubility and increase the usable lifetime of silver, the performance of silver-based reverse osmosis (RO) membranes was assessed by passivating the AgNPs on the coated membranes to Ag/Ag_2S, using Na_2S as a sulfidation agent (Barrios et al., 2020). This resulted in an 85% decrease in silver release rate without compromising the antibacterial performance compared to pristine AgNPs. The silver release rate reduction is due to the protective, low solubility Ag_2S layer forming around the AgNPs (Figure 1) (Barrios et al., 2020). This simple passivation approach allowed the membrane to maintain its silver loading and antimicrobial activity over time, which resulted in improved biofouling control when compared to pristine AgNPs functionalization.

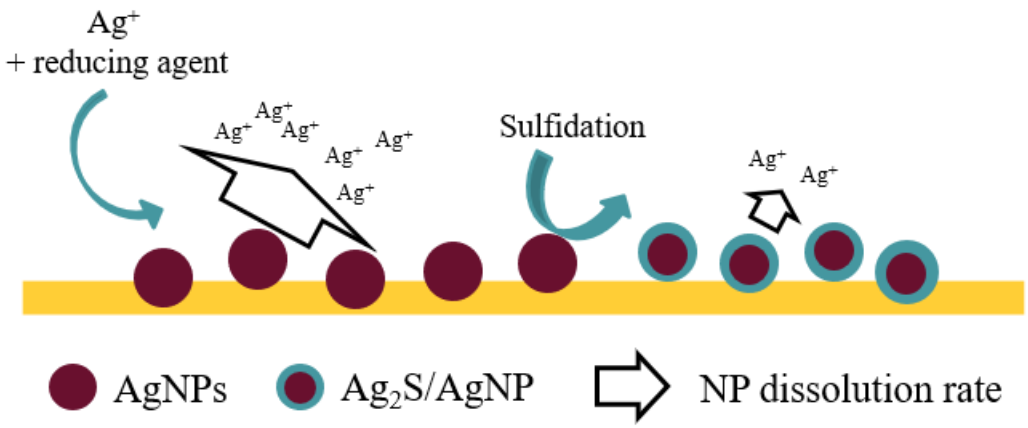

Figure 1: Schematic overview of passivation of AgNPs to core-shell Ag/Ag_2S NPs through sulfidation. A partial Ag_2S layer is formed around AgNPs after sulfidation (Barrios et al., 2020).

This promising biocidal performance of the Ag/Ag_2S coated RO membranes, together with the significant reduction of Ag release, raise the question of whether this method will perform competently on other surfaces (Barrios et al., 2020). At present, the inner surface of majority of ¼-inch pipes used in the drinking water distribution systems, water storage tanks, and even the inner surface of bellow tanks in the ISS is made of stainless steel (Muirhead et al., 2020; Peterson & Callahan, 2007; Roberts et al., 2007). However, the potential application of this new passivated silver coatings for biofouling control on stainless steel has not been demonstrated. In addition, while Ag_2S has shown promising results for the control of silver release without loss of antimicrobial performance, other passivation chemistries exist that may offer similar or even improved performance compared to the very low solubility (K_{sp} = 8×10^{-51}) Ag_2S form. More moderate passivation strategies based on silver-halide structures such as silver bromide (AgBr) and silver iodide (AgI), with K_{sp} of 5.35×10^{-13} and 8.52×10^{-17}, respectively, have proven to have good antimicrobial performance when tested in suspension assays (Liu et

al., 2015; Suchomel et al., 2015). These alternative passivation strategies, by providing an intermediate solubility form between Ag^0 and Ag_2S, have the potential to provide higher biofouling control performance when applied to stainless steel.

In this thesis, we present a stable antibacterial silver coating that can be applied *in situ* on stainless steel surfaces in water storage and distribution systems such as the one used in the ISS. The SS surface was modified by the generation of AgNPs on the surface, and their subsequent treatment to create different forms of passivated silver including Ag_2S, AgBr, or AgI, which are less soluble compared to zerovalent AgNPs. These different forms of silver were compared to determine which form of silver passivation provides the best biofouling resistance while retaining its silver loading on the surface. Antibacterial, biofouling, and silver release assays suggest that Ag/Ag_2S coatings display better long-term bactericidal performance than Ag/AgBr and Ag/AgI coatings while showing a desirable reduction in silver release rate. These simple coatings can be applied on SS without needing to disassemble the system, which makes them well adapted to space conditions, where simple chemistry and processes are preferred.

1.2 Research Question, Hypothesis and Objectives

According to the information available, the primary question that arises is whether this passivation technique will have the same outcome on the stainless steel surface and whether other materials can be used in this method and deliver a similar effect.

The main hypotheses of this project were:

1. By optimizing the Ag:S ratio, the solubility of nanosilver coatings on stainless steel can be significantly reduced without compromising their anti-biofouling properties.

2. Other passivation chemistries exist that can extend the silver release duration and preserve the antibacterial performance of the SS surface which may offer similar or even improved performance compared to Ag_2S passivation.

The following research objectives were pursued to verify the above hypotheses:

1. Form AgNP, Ag/Ag_2S, Ag/AgBr, and Ag/AgI nanoparticles on stainless steel.
2. Characterize the surface of stainless steel before and after functionalization.
3. Perform antibacterial experiments to assess bacterial inactivation by silver-functionalized stainless steel surface.
4. Develop biofilm on functionalized surfaces.
5. Determine the effect of passivation ratio in slowing down the biofilm formation over time.
6. Quantify and compare the percentage of silver released from coatings with different Ag:S and Ag:Br ratios over time.

CHAPTER 2

BACKGROUND LITERATURE

2.1 Applications of silver as a biocide

Silver has long been valued because it is applied for a variety of medical purposes. Herodotus, who is often referred to as "The Father of History", stated that Persian kings, including Cyrus the Great, used to store and transport water in silver vessels to disinfect and purify water (Alexander, 2009; Sim et al., 2018). Historians speculate that silver was probably first used as an antimicrobial wound dressing by the Macedonians to treat wounds and prevent infections before the common era (Alexander, 2009). In the early 1800s, medical staff and scientists began to use silver as an antiseptic for post-surgical infections in dentistry and medical devices (Melaiye & Youngs, 2005). In the last few decades, silver has gained popularity and has been used in a wide range of applications as an antibacterial agent. Other than their applications in clinical devices and biomedical products, AgNPs (1 nm – 100 nm in size) are also used as disinfectants in personal care products, water, air, food packaging, jewelry, and textiles (Deshmukh et al., 2019).

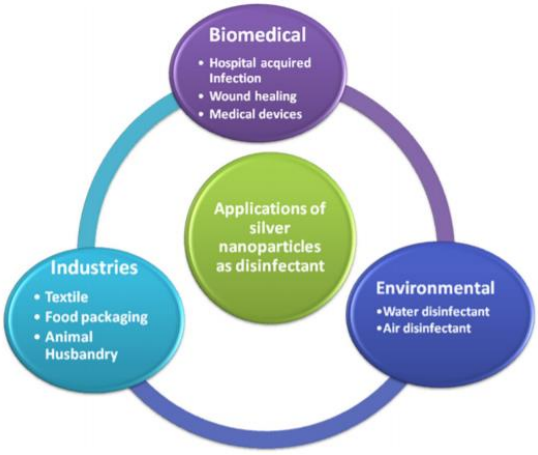

Figure 2: Applications of AgNPs as antimicrobial agents in different sectors (Deshmukh et al., 2019).

2.2 Toxicity of silver nanoparticles

Although the antimicrobial activity of AgNPs has proved to be highly effective against aerobic, anaerobic, Gram-positive, and Gram-negative bacteria as well as more than 650 other microorganisms including fungi and viruses, the exact mechanism of their mode of antimicrobial action is still unknown and is not fully elucidated (Dakal et al., 2016; Konop et al., 2016; Roy et al., 2019). The toxicity of AgNPs and their main method of antimicrobial action on microorganisms did not attract researchers' attention only until recently (Burdușel et al., 2018; Marambio-Jones & Hoek, 2010). Regardless, several studies have been conducted over the last decade in order to fully monitor and understand how AgNPs interact with bacteria cells (Marambio-Jones & Hoek, 2010). Since antimicrobial and characterization assays of AgNPs are not standardized, some investigations have reported results that are contradictory to each other (Vazquez-Muñoz et al., 2017). However, the three most common and possible antimicrobial actions that have been suggested so far are: 1) Direct destruction of membrane and cell wall by AgNPs, 2) Intracellular penetration caused by AgNPs followed by the destruction of intracellular structures, 3) Increased production of reactive oxygen species (ROS) and causing oxidative stress (Dakal et al., 2016; Roy et al., 2019).

The cell membrane of microorganisms is negatively charged due to the presence of sulfur-containing proteins and amino acids inside and outside the membrane (Deshmukh et al., 2019). The positively charged silver ions that are released from AgNPs upon contact and under aerobic conditions, attract the negatively charged sulfur in the cell membrane. This electrostatic attraction facilitates the adhesion of silver ions onto the cell membrane which further leads to the diffusion and uptake of the cell membrane (Bapat et al., 2018;

Dakal et al., 2016; Hsueh et al., 2015). Once silver ions penetrate the cell, they attach to and inactivate metabolic enzymes that provide energy to the cell. This stops the transfer of nutrients, suffocating the cell. Besides, silver ions increase the production of reactive oxygen species which damages cell metabolism and reduce cells' ability to survive. Furthermore, DNA loses its replication capability that eventually leads to the cell's death (Hsueh et al., 2015; Morones et al., 2005; Roy et al., 2019). Finally, all the cellular contents will leak into the environment due to the destruction of the cell wall, which is believed to be the key toxicity mechanism of AgNPs (Dakal et al., 2016; McQuillan et al., 2012).

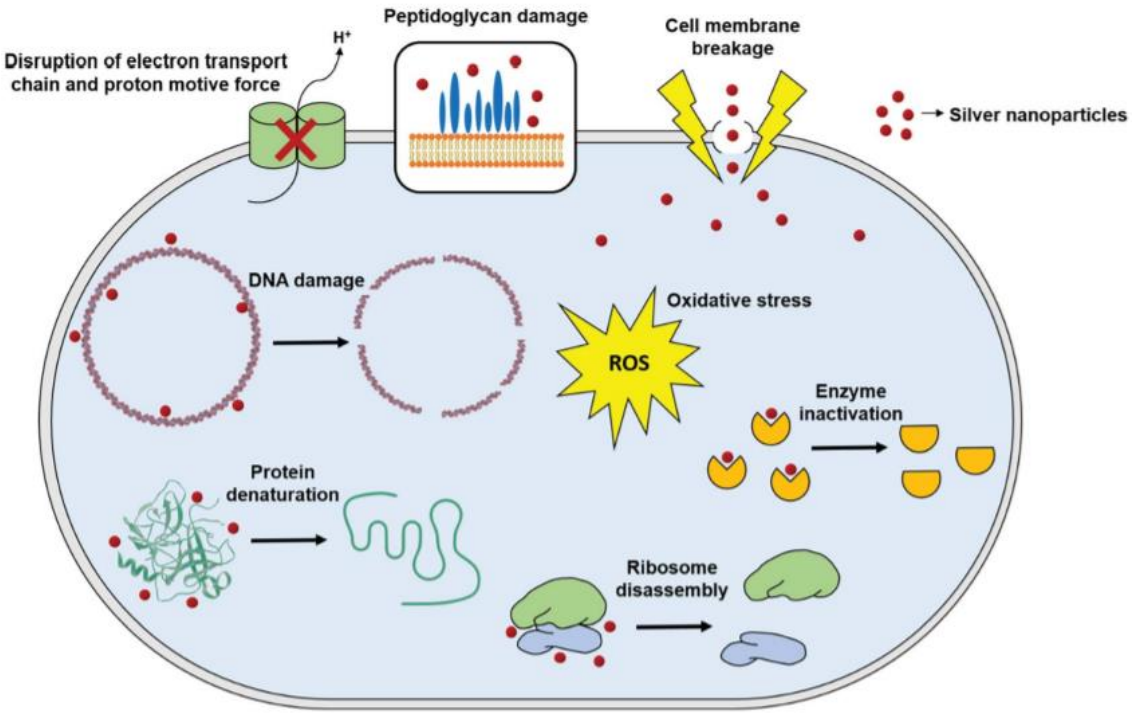

Figure 3: Most prominent mechanisms of antimicrobial action of AgNPs (Roy et al., 2019).

2.3 Factors impacting the antimicrobial action of silver nanoparticles

Physical and chemical properties play an important role in changing the antimicrobial performance of AgNPs Size, shape, surface area, surface charge, concentration, and solubility are among the physicochemical characteristics that can affect the antimicrobial action of AgNPs (W. Li et al., 2018; Roy et al., 2019). Research has revealed that AgNPs with smaller sizes act better and are more toxic against microorganisms (Choi & Hu, 2008). Smaller nanoparticles have a higher surface area which provides a higher interaction area and accelerates the release of silver ions (Roy et al., 2019).

The release of silver ions also depends on the shape of AgNPs as it directly alters the surface area. Previous studies reported that AgNPs with hexagonal or octahedral shapes displayed the highest antimicrobial activity while triangular-shaped particles showed the lowest toxicity (Roy et al., 2019). On the contrary, some scientists publicized that the size or shape of the AgNPs did not significantly impact their biocidal performance (Actis et al., 2015). Therefore, additional research is still needed to fully understand and verify these statements.

Solubility of the silver has a direct relationship with the rate of ionic silver release and thus, governs the antimicrobial action. Silver compounds such as silver nitrate ($AgNO_3$) and silver fluoride (AgF) are among the most soluble while silver sulfide (Ag_2S) and silver arsenate (Ag_3AsO_4) are the least soluble silver forms (W. Li et al., 2018).

Concentration is another property that can impact the antimicrobial performance of silver. Certain investigations suggest that the bactericidal concentration of AgNPs is not consistent and particularly depends on the type of bacteria strain (Singh et al., 2014). Other

environmental conditions also influence the antimicrobial activity of these particles as Chitra *et al* formerly reported that at lower pH's, the nanoparticle surfaces are less negatively or positively charged, which satisfies the adhesion of silver to the negatively charged bacteria (Chitra & Annadurai, 2014). All these key physicochemical characteristics of AgNPs must be taken into account before utilizing them as a disinfectant in different applications.

2.4 Silver as an alternative biocide in space applications

It has been more than fifty years since the Apollo 11 spacecraft landed humans on the moon for the first time. Over the last five decades, the advancement of technology has helped us tremendously to broaden our knowledge about space exploration, and humanity's space-based capabilities have grown significantly since 1969. With the advancement of technology, the duration of space shuttle missions has gradually extended and NASA is looking forward to longer-duration spaceflights and traveling deeper into space eventually (Institute of Medicine (IOM), 2001).

One of the major challenges that astronauts are facing in the International Space Station is microbial contamination, biofilm formation, and the potential health risks that are associated with them. Therefore, space agencies including NASA, ESA (European Space Agency), and JAXA (Japan Aerospace Exploration Agency) are continuously seeking methods to monitor, control, and mitigate biofilm formation in order to protect the space crew from the risk of infection during future space exploration missions (Kim, Tengra, Young, et al., 2013; Yamaguchi et al., 2014; Zea et al., 2020).

The first study on biofilm formation in space was published in 1999 (McLean et al., 2001). Before that, however, more than 100 microorganisms had been previously

identified and isolated from water recycling systems in the Soviet Salyut 6 and 7 and the former Mir space station by scientists (Klintworth et al., 1997; Leys et al., 2009). These challenges still continue after all these years and biofilms are still present and have been detected on different surfaces in the International Space Station, especially in the water recovery system (WRS) which consists of two parts, the Urine Processor Assembly (UPA) and the Water Processor Assembly (WPA), which purify human urine and hygiene waste and recycle them into potable water with more than 74% recovery (Yamaguchi et al., 2014; Yang et al., 2018; Zea et al., 2020). More importantly, it is critical to find an effective disinfectant as a surface coating that can be applied *in situ* in water systems of ISS without the need of disassembly, and that can minimize microbial growth especially because the cost of water is very high and approximately $83,000 per gallon (Aeronautics, n.d.).

Currently, the American side of the ISS uses iodine (I_2) in their potable water system as a disinfectant, whereas the Russian side has been using silver to disinfect their water supplies since the operation of the Russian Mir Space Station (Birmele et al., 2020). Iodine has high initial Total Organic Carbon (TOC), eventually accumulates in the thyroid, and must be removed from the water supply before being consumed by the space crew (Birmele et al., 2012; W. Li et al., 2018; Roberts et al., 2007). Compared to this traditional disinfectant, silver is emerging as a potential disinfectant because of its capacity to inactivate microorganisms without leaving toxic disinfection residues and is highly effective even below 500 parts per billion concentration which is the concentration limit in water that is safe for human consumption (Birmele et al., 2020; Silvestry-Rodriguez et al., 2008). Since the 1980s when it was first introduced in the Russian space stations, this potent biocide has positioned itself as the preferred disinfectant because of its ability to

control microbial growth (Q. Li et al., 2008; Williamson & Emmert, 2013). These significant drawbacks of iodine have led NASA to consider replacing silver as an alternative antimicrobial additive for future space missions (Birmele et al., 2020; Yang et al., 2018).

CHAPTER 3

MATERIALS AND METHODS

3.1 Materials and chemicals

Silver nitrate ($AgNO_3$), sodium borohydride ($NaBH_4$), sodium sulfide (Na_2S), sodium nitrate ($NaNO_3$), Isopropyl alcohol (IPA), sodium phosphate dibasic (Na_2HPO_4), potassium chloride (KCl), D-glucose monohydrate ($C_6H_{14}O_7$), and potassium bicarbonate ($KHCO_3$) were purchased from Sigma Aldrich (St. Louis, MO). Potassium phosphate monobasic (KH_2PO_4), 20 mM propidium iodide (PI), 3.34 mM SYTO 9 nucleic acid stain, and agar were purchased from Fisher Scientific (Waltham, MA). Ammonium chloride (NH_4Cl) and magnesium sulfate heptahydrate ($MgSO_4$) were purchased from ACROS Organics (Columbus, OH). Luria-Bertani (LB) broth and nitric acid (HNO_3) were purchased from VWR International (Radnor, PA). Sodium chloride (NaCl) was purchased from Carolina (Burlington, NC). All the required materials and chemicals were of ACS grade or higher except trace metal grade HNO_3. The 444 stainless steel (SS), a corrosion-resistant form of stainless steel containing between 2 – 3% molybdenum used as a model surface for treatment in the potable water systems of the International Space Station (ISS) was provided by Cactus Materials, Inc. (Tempe, AZ) and used in all the observations. All the solutions were made and surfaces were washed using deionized (DI) water from a Barnstead^{TM} GenPure xCAD Plus Ultrapure Water Purification System (Thermo Scientific, Waltham, MA).

3.2 In situ formation of silver nanoparticles

Coupons of stainless steel 444 (1cm × 1cm) were soaked in a 20% isopropanol solution for 20 minutes and rinsed 3 times in DI water. Then, they were placed in 50 mL Eppendorf tubes and submerged in a DI water solution containing 300 mM silver nitrate ($AgNO_3$) and agitated for 20 minutes. Subsequently, the $AgNO_3$ solution was removed from the tubes and functionalized coupons were rinsed in DI water, and a 300 mM concentration of sodium borohydride ($NaBH_4$) solution was added to the tubes as a reducing agent, and tubes were agitated for 5 minutes to nucleate the Ag^+ ions to AgNPs on the SS surface following the previously developed protocol (Barrios et al., 2020; Ben-Sasson et al., 2014).

3.3 Passivation of silver nanoparticles

The previously prepared AgNP-modified surfaces were rinsed in DI water to separate loosen or weakly attached AgNPs from the SS surface. During the sulfidation, bromidation, or iodization procedures, the AgNP-functionalized SS surfaces were introduced to a DI water solution containing 0.01 M $NaNO_3$ (constant) with different concentrations of either sodium sulfide (Na_2S), sodium bromide (NaBr), or sodium iodide (NaI) ranging from 10^{-5}, 10^{-3}, and 10^{-1} M. The samples were agitated for 24 h to form an Ag_2S, AgBr, or AgI layer around the AgNPs and to generate Ag/Ag_2S – Ag/AgBr – Ag/AgI NPs of different Ag:S – Ag:Br – Ag:I ratios.

3.4 Characterization of functionalized stainless steel surfaces

Contact angles (CA) were analyzed on an Attension Theta by Biolin Scientific (Gothenburg, Sweden) using a 1001 TPLT Hamilton syringe (Reno, NV). At least 6

different CA measurements were taken per sample from different areas of the pristine and functionalized SS to account for variability. The software recorded ~200 data points over 10 seconds for each measurement (18 megaohm DI water). Subsequently, CA values were averaged and documented as a final mean and presented as average ± standard deviation (Barrios et al., 2020).

The surface roughness of pristine and Ag-modified SS coupons was measured by atomic force microscopy (AFM). AFM was carried out using tapping mode with a Bruker Multimode 8 AFM (Digital Instruments, Plainview, NY) equipped with an NCHV (Bruker, Camarillo, CA. Roughness parameters were analyzed using the Bruker NanoScope Analysis version 1.9 software.

The zeta potential of the stainless steel surface was assessed by streaming potential measurements using a ZetaCAD analyzer with a flat surface cell (CAD Instruments, Les Essarts-le-Roi, France). An electrolyte solution containing 5 mM KCl and 0.1 mM HCO_3 was used throughout the analysis. Measurements were conducted over a pH range of 4 – 10 with a pressure range from 30 – 70 psi, and step durations of 30 and 60 seconds following previously published procedures (Barrios et al., 2020; Rice et al., 2018).

Morphology and elemental identification of the SS surface were characterized using scanning electron microscopy (ESEM-FEG XL-30, Philips Hitachi SU-70, Hillsboro, OR) at an acceleration voltage between 5 – 25 kV. Energy-dispersive X-ray (EDX) analyses were conducted to detect silver, sulfur, bromine, and iodine on the SS surface.

3.5 Antibacterial activity of functionalized stainless steel

Pseudomonas aeruginosa (ATCC 25668), a biofilm-forming bacterial model, was employed in this project to evaluate the antibacterial performance of silver-functionalized SS substrates in static antimicrobial experiments. Bacteria cultures were kept in enclosed LB agar Petri dishes and stored at 4°C in the refrigerator. *P. aeruginosa* was grown overnight in 50 mL LB broth placed in a Barnstead orbital incubator shaker at 37°C and rotating at 140 rpm. Subsequently, bacteria solution was diluted in fresh LB (1:25) while maintaining the same conditions used in the previous procedure for 2 h until cell culture reached to an optical density of 1.0 at 600 nm. Portions of bacteria cells were washed 3 times with 0.9% NaCl solution in 1 mL Eppendorf tubes by centrifugation for 1 minute at 5000 rpm to separate bacteria culture from LB broth and to withdraw the cell remains. Pristine and functionalized 444 SS coupons were deposited in 50 mL falcon tubes and were then exposed to a suspension of *P. aeruginosa* (10^7 Colony Forming Units/mL) in simple sterile saline (0.9% NaCl) solution. They were agitated for 3 h at room temperature. The SS coupons were removed from the bacterial suspension and the excess solution was removed by slowly touching the edge of each coupon on a clean kimwipe paper. Coupons were then added to new tubes containing 10 mL of 0.9% NaCl solution and bath sonicated for 10 minutes to desorb the attached cells. The collected cells were diluted, plated on LB agar plates, and incubated overnight at 37°C to count the number of viable colony forming units (CFU).

3.6 Quantification of silver release rate

Prepared coupons of functionalized 444 SS were weighed to serve as a measure of the total sample mass/surface area and then placed in sealed acid-washed (trace metal-free) 50 mL polypropylene tubes. A 4.15 mL volume (used for 1 cm × 1 cm coupon) of DI water solution was placed in the tubes and the tubes were each labeled and sealed. Tubes were continuously agitated using an orbital shaker for 4 h time points. After the 4 h contact time, SS coupons were removed and dried by placing the corner of each sample on a kimwipe paper. Once the coupons were removed and dried after the 4 h contact time, 70% trace metal grade HNO_3 was added to a final concentration of 10% in each tube to quantify the amount of silver leached to the water. Dried coupons were then placed in a new set of tubes. This time, the solution inside the tubes had already been acidified and contained 0.85 mL of 70% HNO_3 and 4.15 mL DI water. Samples were agitated for 24 h and afterward, quantification was done by Inductively coupled plasma mass spectrometry (ICP-MS).

3.7 Biofilm development on functionalized stainless steel

Biofilm formation was monitored using a microscopy flow cell designed to hold pristine and silver-modified coupons of the specified size (1 cm × 1 cm). Initially, bacteria were added in a sterile glass flask containing 50 mL LB broth, incubated in a Barnstead orbital incubator shaker, and were grown overnight at room temperature. Bacteria suspension was then diluted in LB broth (1:25) and placed inside the orbital incubator shaker for an additional 2 – 3 h. Once the cell culture reached an optical density of 1.0 at 600 nm, aliquots of bacterial cells were washed 3 times following the previously established procedure. A peristaltic pump was used to circulate a synthetic growth medium

(M9 minimal medium) supplemented with *P. aeruginosa* (2×10^7 Colony Forming Units/mL). Fresh synthetic growth medium was made by supplementing 6 g of sodium phosphate dibasic (Na_2HPO_4), 3 g of potassium phosphate monobasic (KH_2PO_4), 0.5 g of sodium chloride (NaCl), 1 g of ammonium chloride (NH_4Cl) in 1 L of DI water and autoclaving it. Once media was autoclaved, 1 mL of 1M magnesium sulfate ($MgSO_4$), 1 mL of 0.1M calcium chloride ($CaCl_2$), and 20 mL of 10% (w/v) glucose were added, and then stirred on a stirrer. All three ingredients were prepared in a sterile environment before being added to the solution.

In all the experiments, two coupons of the specified size of each sample were placed in the flow cell in every experiment. The synthetic growth medium was poured into a modified plastic beaker placed inside a secondary container to avoid any possible contamination in case of spills. Bacteria suspension was then recirculated inside the flow cell using a peristaltic pump (Masterflex) at a constant flow rate of 3.2 mL min^{-1} for 120 h, which resulted in the formation of biofilm on the surface of SS coupons. Subsequently, the length of biofilm on the surfaces was quantified using Optical Coherence Tomography (OCT) microscope (Ganymede II, Thorlabs, Germany) and ImageJ analysis of biofilm.

3.8 Data analysis and statistics

All experiments were performed in at least three independent replicates (n = 3). The standard deviation in each experiment was calculated and the results were standardized relative to the control. By performing a one-way analysis of variance ANOVA, followed by a Tukey post hoc test using OriginPro 2018 software, statistical differences between the

control and Ag-functionalized samples were obtained, with a p-value of less than 0.05 acknowledged as being significant.

CHAPTER 4

RESULTS AND DISCUSSION

4.1 Stainless steel surface characterization

The functionalization of the SS surface was validated by both SEM microscopy and XPS (Appendix A). The functionalization procedure was performed in two steps: 1) in situ formation of AgNPs on the SS surfaces and 2) functionalization of AgNPs by sulfidation or halogenation. Silver nitrate and a reducing agent ($NaBH_4$) are the only two reagents that are used in the first step; the second stage requires sulfidation (sodium sulfide) or halogenation (sodium bromide and sodium iodide) agents. Once the first stage was completed and AgNPs were formed on the SS surface, different solutions comprising different concentrations of Na_2S, NaBr, or NaI were put in contact with the samples to form Ag: Ag_2S, Ag: AgBr, or Ag: AgI particles on SS surface.

Figure 4 exhibits SEM images of pristine SS, AgNP-modified SS, sulfidized SS, bromidized SS and iodized SS (Figure 4A-E). All the images represent the flat and smooth surface of stainless steel, however, the difference between the pristine and coated surfaces of SS is evident. Image C, D, and E show the small AgNPs on the SS surface. Image (C) clearly shows that the surface is entirely covered by NPs after sulfidation without any signs of particle agglomeration. Conversely, images (D) and (E) show fewer AgNPs on the surface, and there are evident signs of agglomeration. The uniform surface coverage of AgNPs after sulfidation can increase the anti-biofouling properties of the surface as the particles are more stable and have a higher surface area when the surface is evenly covered.

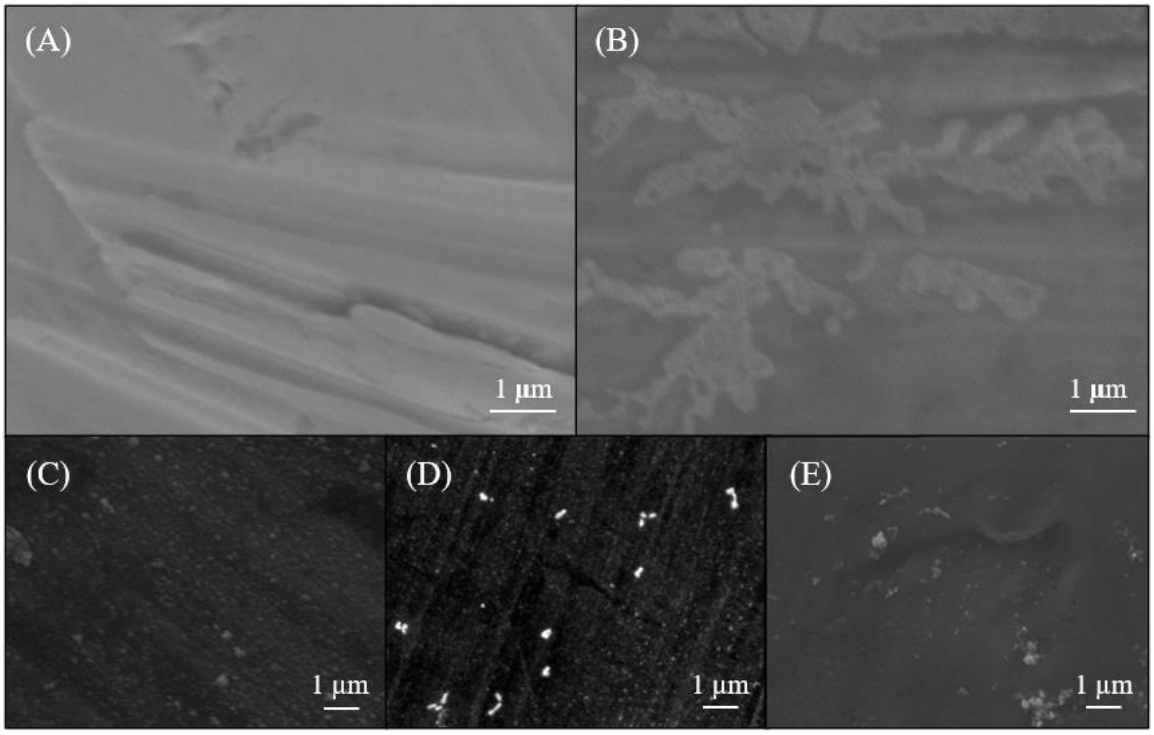

Figure 4: Functionalized stainless steel characterization. Scanning electron microscopy imaging of A) control, B) AgNPs functionalized, C) sulfidized AgNPs, D) bromidized AgNPs, and E) Iodized AgNPs stainless steel. All images were taken at a scale of 1um. Concentrations of 10^{-1} M Na2S, 10^{-1} M NaBr, and 10^{-1} M NaI were used to passivate AgNPs in A, B, and C images, respectively.

4.2 Silver nanoparticles passivation improves the antibacterial activity

The Ag^{+} ion is known to be the main driver for the toxicity of AgNPs to bacteria (Xiu et al., 2012). Therefore, reducing Ag^{+} release can also reduce the antimicrobial properties of the AgNPs on the stainless steel surface. Previous studies have shown that highly sulfidized Ag_2S NPs have low toxicity to *P. aeruginosa* and *Escherichia coli* (Barrios et al., 2020). However, Barrios et al showed that it is possible to partially sulfidize AgNPs and achieve a slower release rate without significantly impacting antimicrobial activity (Barrios et al., 2020).

To determine the passivation conditions that can achieve this balance between silver release and bacterial inactivation for the different passivation chemistries considered, pristine and functionalized SS coupons coated with AgNPs, Ag:Ag_2S, Ag:AgBr, and Ag:AgI of different passivation extents were placed in a suspension of *P. aeruginosa* which was selected as a biofilm-forming bacteria model as it has been repeatedly identified in the International Space Station over the years (Birmele et al., 2012; Kim, Tengra, Shong, et al., 2013; Zea et al., 2020). After 3 h of contact, bacteria cells were detached from the surface and incubated to quantify the number of viable CFU. Figure 3 shows the average viable CFU counts on each sample relative to the control. CFU count decreased to 60.95 ± 23.72, 41.24 ± 17.86, 30.3 ± 12.3, and 25.17 ± 11.26% for coupons functionalized with AgNPs or AgNPs treated with 10^{-1}, 10^{-3}, and 10^{-5} M Na_2S, respectively. All three Na_2S concentrations confirm the effectiveness of silver sulfidation in reducing the number of viable CFU. All the sulfidized samples except for the 10^{-1} M Na_2S diminished *P. aeruginosa* CFU count on SS in a statistically significant way, similar to the previously obtained results for reverse osmosis (RO) membranes (Barrios et al., 2020).

A similar trend is observed for bromidized and iodized AgNPs (Figure 5). After 3 h of contact time, viable CFU counts for the AgNPs treated with 10^{-1}, 10^{-3}, and 10^{-5} M NaBr decreased to 60.53 ± 8.74, 47.98 ± 17.46, and 59.34 ± 19.23% compared to the control, respectively, while for the NaI-treated samples with same passivation concentrations, the viable CFU count decreased to 60.8 ± 23.3, 47.16 ± 25.61, and 38.66 ± 13.43%, respectively. Results demonstrate that there is no statistical difference between bromidized or iodized samples and the AgNP-functionalized stainless steel. When compared at the same molar concentrations of passivating agents, all sulfidized AgNPs

showed slightly lower numbers of viable CFUs compared to bromidized and iodized AgNPs, with the 10^{-3} M and 10^{-5} M Na_2S passivation treatment having the best static antimicrobial performance with a 70 – 75% decrease in viable CFU on the surface, compared to the control sample.

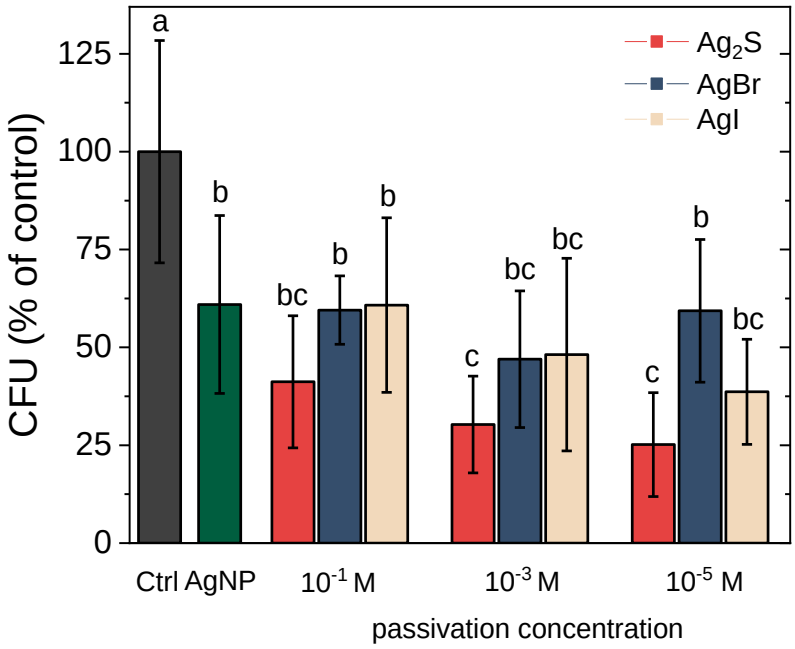

Figure 5: Number of viable colony forming units (CFU) on SS coupons after 3 hours of contact with a 10^7 CFU/mL *P. aeruginosa* suspension at room temperature. Grey, green, blue, orange and yellow columns represent control, AgNP, sulfidized, bromidized, and iodized coupons respectively. 10^{-1} M, 10^{-3} M and 10^{-5} M in the X-axis represent the passivation concentration that was used in the functionalization process. Results were normalized with respect to the control (n=5).

4.3 Silver nanoparticles passivation slows down biofilm formation

Silver iodide was not tested in additional experiments due to its poor performance against silver sulfide and also because of its adverse effects on human health and also imparting a bad taste to drinking water as previously reported by NASA (Birmele et al., 2020; Roberts et al., 2007). Biofouling experiments were carried out to measure the

thickness of biofilms on pristine and silver-modified stainless steel surfaces over time. Surfaces were continuously in contact with M9 minimal medium containing *P. aeruginosa* suspension (2×10^7 CFU mL^{-1}) for 5 days and with constant recirculation. Figure 6 demonstrates that the length of the biofilm formed on the surface of AgNP, 10^{-1} M, 10^{-3} M, 10^{-5} M Na_2S and 10^{-1} M, 10^{-3} M, 10^{-5} M NaBr functionalized coupons was reduced to 53.69 ± 12.08, 53.38 ± 7.8, 29.83 ± 6.97, 43.11 ± 15.69, 36.33 ± 12.47, 29.9 ± 9.07, and 53.38 ± 20.01% respectively, compared to the control sample. ImageJ analysis of biofilm length on the fifth day of exposure suggests that sulfidized and bromidized SS samples demonstrate a similar or even improved biofouling resistance compared to AgNP-coated samples. Less biofilm was formed on the surface of SS coupons with 10^{-3} M Na_2S and 10^{-3} M NaBr concentrations compared to the surface of AgNP impregnated coupons. This can be explained by the fact that sulfidation slows down the dissolution of AgNPs and therefore, silver remains at a higher concentration on the surface for a longer time, which allows for better biofouling mitigation. On the other hand, 10^{-1} M Na_2S and 10^{-1} M NaBr concentrations form a thicker passivation shell around the AgNPs which limits its antibacterial performance when compared to the 10^{-3}M concentration.

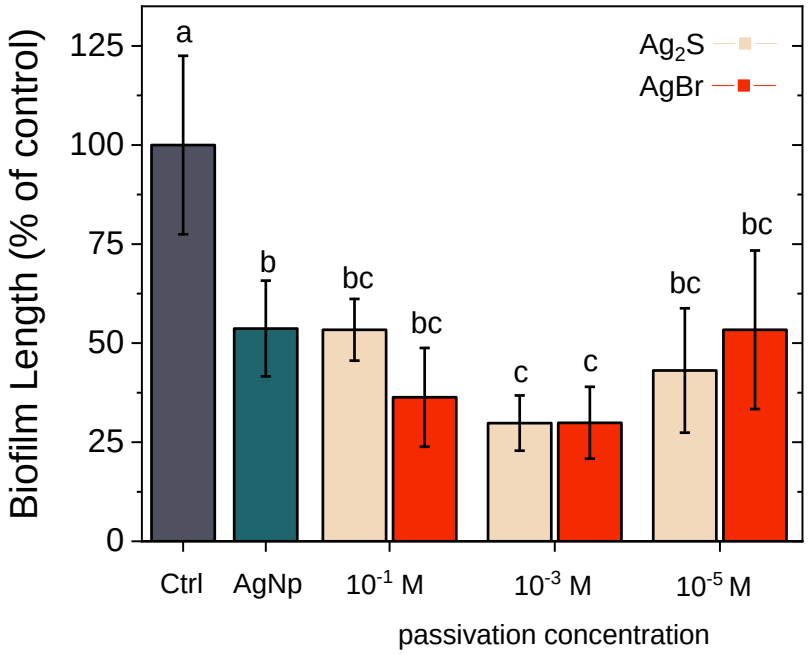

Figure 6: Biofilm length (mm) on the surface of pristine and silver-modified SS coupons after 5-day exposure to M9 minimal medium with a 2×10^7 *P. aeruginosa* concentration in an electrochemical cell set-up. Results have been normalized with respect to control.

These results indicate that both AgBr and Ag_2S-modified SS surfaces can reduce biofilm formation, however, there is a threshold of sulfidation and bromidation (10^{-3} M concentration) that proves to be more effective in slowing down the formation of biofilm on the SS surface for extended periods of time.

4.4 Silver nanoparticles passivation decelerates silver release

The release of Ag^+ from AgNPs is an extremely important factor to consider in space missions as it partly controls the long-term biofouling performance of the surface. The formation of low-solubility forms of silver (Ag_2S, AgBr) around AgNPs is expected to reduce silver release from the functionalized stainless steel surfaces, as it was shown previously for membranes (Barrios et al., 2020) and polymers (Sambhy et al., 2006). Based

on the K_{sp} of the different forms of silver generated, the silver release rate should decrease in the order of AgBr > Ag_2S. However, the total silver release may differ from this order due to potential partial passivation of the AgNPs on the surface. Therefore, silver release was quantified for the different passivated surfaces to assess the effectiveness of each passivation strategy in retaining the silver on the surface over time.

Figure 7. depicts the total percentage of silver released from stainless steel coupons functionalized by pristine AgNPs, and AgNPs passivated with 10^{-1} M, 10^{-3} M, 10^{-5} M Na_2S and NaBr. Sulfidation was found to decrease the percentage of silver released after 4 h from 16.23 ± 3.88% for AgNP-treated samples to 0.72 ± 0.49, 2.91 ± 1.72, and 2.24 ± 1.86% for 10^{-1} M, 10^{-3} M, and 10^{-5} M Na_2S-treated samples, respectively. For the bromidized samples the silver release percentage reduced to 3.25 ± 1.73, 2.02 ± 1.44, and 2.25 ± 1.24% for 10^{-1} M, 10^{-3} M, and 10^{-5} M NaBr-treated samples, respectively. These results are in agreement with similar silver release experiments and confirm the effect of sulfidation in slowing down the Ag release process (Barrios et al., 2020; Lee et al., 2016; Levard et al., 2011; Sambhy et al., 2006)

When the two strategies are compared, no statistical difference is found between sulfidized and bromidized samples and both passivation techniques show a significant reduction in the percentage of Ag released after 4 h compared to AgNP-treated samples.

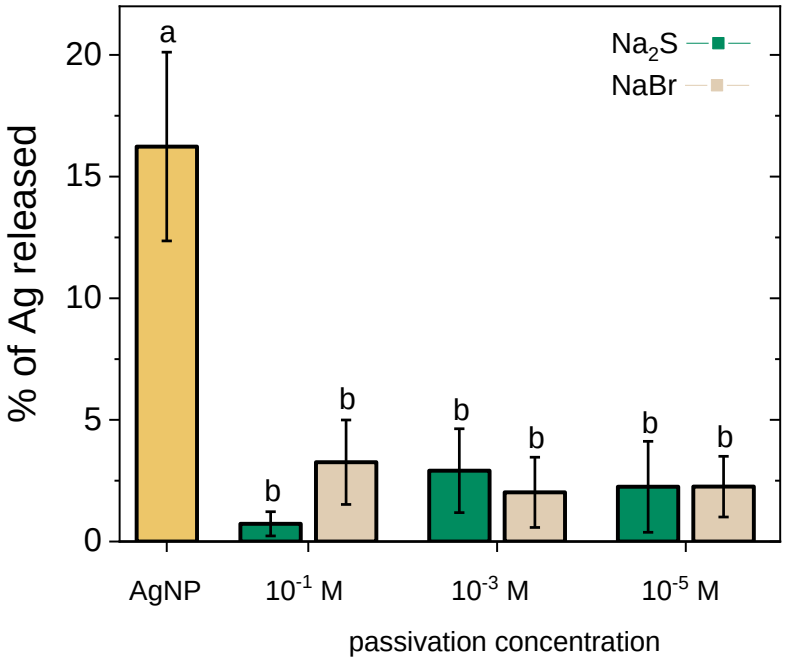

Figure 7: Percentage of silver released from AgNP, sulfidized and bromidized samples after 4 h agitation in a DI water solution. Ag was quantified using ICP-MS. Different letters indicate statistical difference ($p < 0.05$) $n = 3$.

4.5 Functionalization effects on the surface properties

Surface functionalization can change the fouling tendency of any surface. Therefore, it is of paramount importance to assess how these divergent modifications of silver can alter the surface characteristics with respect to the pristine stainless steel. The zeta potential of stainless steel samples slightly decreased to more negative values after functionalization (Figure 8). In addition, the surface zeta potential of functionalized samples follows a similar trend, with the sulfidized SS being slightly less negative compared to the unsulfidized one since the AgNP are more negatively charged (Reinsch et al., 2012). Overall, since most of the surface is still stainless steel even after

functionalization, and stainless steel surface has a negative zeta potential (Wu et al., 2018), the zeta potential of the samples remained negative ranging from 0 to – 20 mV.

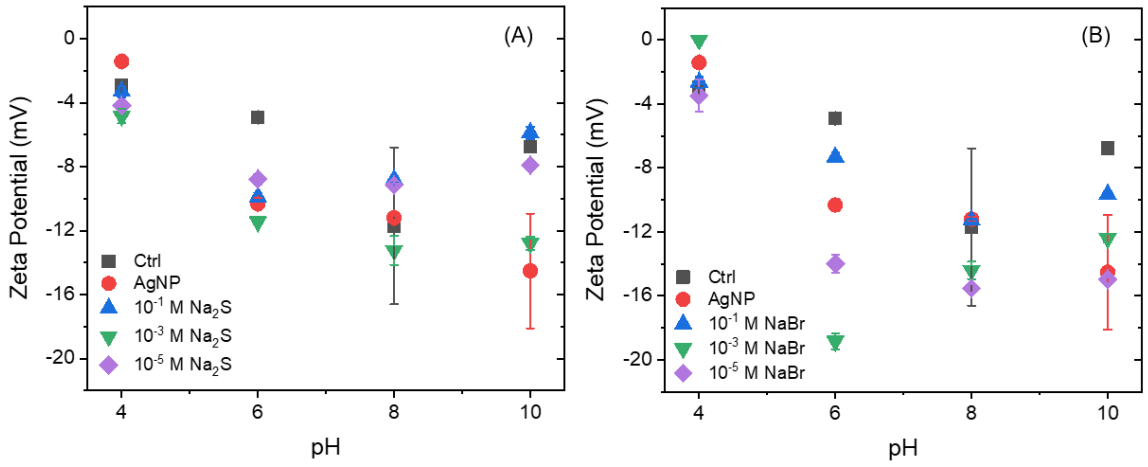

Figure 8: Zeta potential measurements of (A) sulfidized and (B) bromidized samples from pH 4 to pH 10.

Further analysis using AFM imaging indicated that functionalizing SS surface with AgNPs and different concentrations of the less soluble forms of silver (AgBr – Ag_2S) significantly ($p>0.05$) impacts the SS surface roughness when compared to pristine SS. As quantified by AFM, control SS showed an average surface roughness of 30.95 nm ± 5.00, while the treated SS had values of 35.8 nm ± 7.17, 54.02 nm ± 8.56, 61.57 nm ± 1.7, and 36.37 nm ± 4.14 for AgNP, 10^{-1} M, 10^{-3} M, and 10^{-5} M Na_2S-treated samples, respectively. Following, bromidized samples showed an average surface roughness of 50.3 nm ± 11.66, 43.82 nm ± 4.74, and 33.65 nm ± 9.09 for SS surfaces functionalized with 10^{-1} M, 10^{-3} M, and 10^{-5} M NaBr concentrations. Although functionalization did not significantly affect the SS surface roughness of AgNP and bromidized samples, the surface roughness of 10^{-1} M and 10^{-3} M Na_2S-treated coupons increased significantly compared to the control

coupon, and roughness tends to decrease as the Na_2S and NaBr concentration decreases (Figure 9).

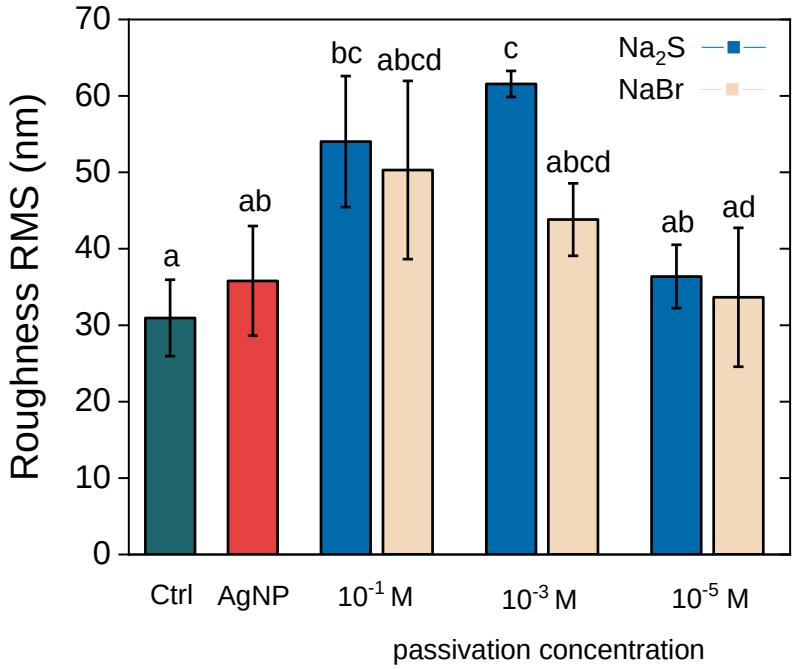

Figure 9: AFM surface roughness (root mean square) parameters of pristine and functionalized stainless steel. Different letters indicate statistical difference ($p < 0.05$) n = 4.

Hydrophobicity/hydrophilicity of SS surfaces was assessed by measuring the water contact angle (CA). Functionalization of SS did not significantly impact the SS hydrophilicity when compared to the control sample, with measured contact angles of 74.99 ± 0.86°, 69.55 ± 2.44°, 68.28 ± 1.64°, 75.94 ± 3.29°, 75.78 ± 2.88°, 66.14 ± 10.49°, 70.48 ± 8.31°, and 76.7 ± 6.23° for the pristine, AgNP, 10^{-1} M Na_2S, 10^{-3} M Na_2S, 10^{-5} M Na_2S, 10^{-1} M NaBr, 10^{-3} M NaBr, and 10^{-5} M NaBr SS samples, respectively. However, when compared together, CA of 10^{-1} M NaBr and 10^{-5} M NaBr were significantly different from each other.

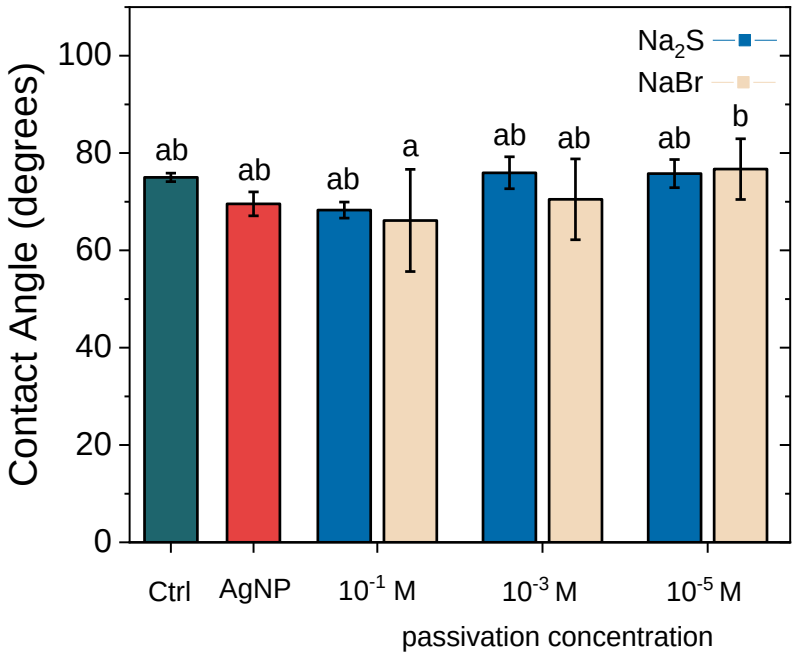

Figure 10: CA of pristine and Ag-functionalized SS measured by surface contact angles. Different letters indicate statistical difference ($p < 0.05$) n = 6.

Therefore, based on the surface characterization results, surface roughness tends to slightly increase by functionalizing the stainless steel with different forms of silver which is due to the agglomeration of AgNPs on the SS surface as shown on the scanning electron microscopy images (Figure 4). Previous studies have shown that there is a positive correlation between surface roughness and the formation of biofilm. However, there are contradictory theories as to whether roughness has a significant impact on bacterial adhesion and biofilm formation on the surface or not (De-la-Pinta et al., 2019). In this research, since both sulfidation and bromidation techniques have shown a considerable increase in anti-biofouling and antibacterial performance of the SS surface, it can be concluded that the higher bactericidal activity and biofouling resistance of silver-impregnated surfaces are mainly due to the inherent biocidal properties of AgNPs attached to the SS surface not the physical properties of the SS surface.

CHAPTER 5

SUMMARY AND CONCLUSIONS

Biofilm proliferation on the inner surface of the International Space Station's WRS is among the most challenging issues that NASA is facing today and this has raised several concerns regarding the potential harms it can cause to astronauts' health. Therefore, NASA is striving to find a permanent solution for this issue to prevent it from occurring in future long-term spaceflights that could range from several months to several years. This study provides insight into how a simple *in situ* nucleation of AgNPs followed by their partial passivation by sulfidation, bromidation, and iodization with different extents can increase the durability, antibacterial performance, and biofouling resistance of stainless steel surface. All three strategies showed bacteria inactivation, however, AgI was not tested in these further investigations due to its drawbacks and lower antibacterial performance. Sulfidation and bromidation of AgNPs reduced biofilm thickness by >70% and significantly decreased the percentage of silver release from 16% for AgNPs to less than 3% and 6%, respectively. In general, sulfidation seems to be the most effective choice for biofouling mitigation on stainless steel as it exhibited the highest antimicrobial activity and durability, and it is also a more preferable option as it does not result in the halogenation of organic compounds as opposed to the other techniques. Future research must be conducted to identify appropriate alternative reagents with a lower toxicity class (<2) that are compatible with space exploration, and to evaluate the effectiveness of sulfidation on other metals including Inconel 718 and Titanium 6AI-4V used in the water distribution systems of International Space Station.

REFERENCES

Actis, L., Srinivasan, A., Lopez-Ribot, J. L., Ramasubramanian, A. K., & Ong, J. L. (2015). Effect of silver nanoparticle geometry on methicillin susceptible and resistant Staphylococcus aureus, and osteoblast viability. *Journal of Materials Science: Materials in Medicine*, *26*(7), 1–7. https://doi.org/10.1007/s10856-015-5538-8

Aeronautics, N. (n.d.). *High Performance Water Recycling System for Space Exploration*. https://sbir.nasa.gov/success-stories/high-performance-water-recycling-system-space-exploration

Alexander, J. W. (2009). History of the medical use of silver. *Surgical Infections*, *10*(3), 289–292. https://doi.org/10.1089/sur.2008.9941

Alissawi, N., Zaporojtchenko, V., Strunskus, T., Hrkac, T., Kocabas, I., Erkartal, B., Chakravadhanula, V. S. K., Kienle, L., Grundmeier, G., Garbe-Schönberg, D., & Faupel, F. (2012). Tuning of the ion release properties of silver nanoparticles buried under a hydrophobic polymer barrier. *Journal of Nanoparticle Research*, *14*(7). https://doi.org/10.1007/s11051-012-0928-z

Bapat, R. A., Chaubal, T. V., Joshi, C. P., Bapat, P. R., Choudhury, H., Pandey, M., Gorain, B., & Kesharwani, P. (2018). An overview of application of silver nanoparticles for biomaterials in dentistry. *Materials Science and Engineering C*, *91*(September 2017), 881–898. https://doi.org/10.1016/j.msec.2018.05.069

Barrios, A. C., Carrillo, D., Waag, T. R., Rice, D., Bi, Y., Islam, R., & Perreault, F. (2020). Prolonging the antibacterial activity of nanosilver-coated membranes through partial sulfidation. *Environmental Science: Nano*, *7*(9), 2607–2617. https://doi.org/10.1039/d0en00300j

Ben-Sasson, M., Lu, X., Bar-Zeev, E., Zodrow, K. R., Nejati, S., Qi, G., Giannelis, E. P., & Elimelech, M. (2014). In situ formation of silver nanoparticles on thin-film composite reverse osmosis membranes for biofouling mitigation. *Water Research*, *62*, 260–270. https://doi.org/10.1016/j.watres.2014.05.049

Birmele, M. N., Morford, M. A., & Roberts, M. S. (2012). Antimicrobial resources for disinfection of potable water systems for future spacecraft. *42nd International Conference on Environmental Systems 2012, ICES 2012*. https://doi.org/10.2514/6.2012-3507

Birmele, M. N., Services, E., Team, C., Contract, E. S., Qna, T., & Space, K. (2020). *Disinfection of Spacecraft Potable Water Systems by Passivation with Ionic Silver*. 1–8.

Burdușel, A. C., Gherasim, O., Grumezescu, A. M., Mogoantă, L., Ficai, A., & Andronescu, E. (2018). Biomedical applications of silver nanoparticles: An up-to-date overview. *Nanomaterials*, *8*(9), 1–25. https://doi.org/10.3390/nano8090681

Chitra, K., & Annadurai, G. (2014). Antibacterial activity of pH-dependent biosynthesized silver nanoparticles against clinical pathogen. *BioMed Research International*, *2014*, 6–11. https://doi.org/10.1155/2014/725165

Choi, O., & Hu, Z. (2008). Size dependent and reactive oxygen species related nanosilver toxicity to nitrifying bacteria. *Environmental Science and Technology*, *42*(12), 4583–4588. https://doi.org/10.1021/es703238h

Dakal, T. C., Kumar, A., Majumdar, R. S., & Yadav, V. (2016). Mechanistic basis of antimicrobial actions of silver nanoparticles. *Frontiers in Microbiology*, *7*(NOV), 1–17. https://doi.org/10.3389/fmicb.2016.01831

De-la-Pinta, I., Cobos, M., Ibarretxe, J., Montoya, E., Eraso, E., Guraya, T., & Quindós, G. (2019). Effect of biomaterials hydrophobicity and roughness on biofilm development. *Journal of Materials Science: Materials in Medicine*, *30*(7). https://doi.org/10.1007/s10856-019-6281-3

Deshmukh, S. P., Patil, S. M., Mullani, S. B., & Delekar, S. D. (2019). Silver nanoparticles as an effective disinfectant: A review. *Materials Science and Engineering C*, *97*(December 2018), 954–965. https://doi.org/10.1016/j.msec.2018.12.102

Hsueh, Y. H., Lin, K. S., Ke, W. J., Hsieh, C. Te, Chiang, C. L., Tzou, D. Y., & Liu, S. T. (2015). The antimicrobial properties of silver nanoparticles in bacillus subtilis are mediated by released Ag+ ions. *PLoS ONE*, *10*(12), 1–17. https://doi.org/10.1371/journal.pone.0144306

Institute of Medicine (IOM). (2001). Safe passage: Astronaut Care for Exploration Missions (Chapter 2). In *Institute of Medicine*. http://www.nap.edu/catalog.php?record_id=10218

Kim, W., Tengra, F. K., Shong, J., Marchand, N., Chan, H. K., Young, Z., Pangule, R. C., Parra, M., Dordick, J. S., Plawsky, J. L., & Collins, C. H. (2013). Effect of spaceflight on Pseudomonas aeruginosa final cell density is modulated by nutrient and oxygen availability. *BMC Microbiology*, *13*(1). https://doi.org/10.1186/1471-2180-13-241

Kim, W., Tengra, F. K., Young, Z., Shong, J., Marchand, N., Chan, H. K., Pangule, R. C., Parra, M., Dordick, J. S., Plawsky, J. L., & Collins, C. H. (2013). Spaceflight Promotes Biofilm Formation by Pseudomonas aeruginosa. *PLoS ONE*, *8*(4), 1–8. https://doi.org/10.1371/journal.pone.0062437

Klintworth, R., Reher, H. J., Viktorov, A. N., & Bohle, D. (1997). Biological induced corrosion of materials: New test methods and experiences from MIR station. *European Space Agency, (Special Publication) ESA SP*, *44*(399), 513–522.

Konop, M., Damps, T., Misicka, A., & Rudnicka, L. (2016). Certain Aspects of Silver and Silver Nanoparticles in Wound Care: A Minireview. *Journal of Nanomaterials*, *2016*. https://doi.org/10.1155/2016/7614753

Lee, S. W., Park, S. Y., Kim, Y., Im, H., & Choi, J. (2016). Effect of sulfidation and dissolved organic matters on toxicity of silver nanoparticles in sediment dwelling organism, Chironomus riparius. *Science of the Total Environment*, *553*, 565–573. https://doi.org/10.1016/j.scitotenv.2016.02.064

Levard, C., Reinsch, B. C., Michel, F. M., Oumahi, C., Lowry, G. V., & Brown, G. E. (2011). Sulfidation processes of PVP-coated silver nanoparticles in aqueous solution: Impact on dissolution rate. *Environmental Science and Technology*, *45*(12), 5260–5266. https://doi.org/10.1021/es2007758

Leys, N., Baatout, S., Rosier, C., Dams, A., s'Heeren, C., Wattiez, R., & Mergeay, M. (2009). The response of Cupriavidus metallidurans CH34 to spaceflight in the international space station. *Antonie van Leeuwenhoek, International Journal of General and Molecular Microbiology*, *96*(2 SPEC. ISS.), 227–245. https://doi.org/10.1007/s10482-009-9360-5

Li, Q., Mahendra, S., Lyon, D. Y., Brunet, L., Liga, M. V., Li, D., & Alvarez, P. J. J. (2008). Antimicrobial nanomaterials for water disinfection and microbial control: Potential applications and implications. *Water Research*, *42*(18), 4591–4602. https://doi.org/10.1016/j.watres.2008.08.015

Li, W., Calle, L. M., Hanford, A. J., Stambaugh, I., & Callahan, M. R. (2018). Investigation of Silver Biocide as a Disinfection Technology for Spacecraft – An Early Literature Review. *48th International Conference on Environmental Systems, July 2018*, ICES-2018-82.

Liu, Z., Guo, W., Guo, C., & Liu, S. (2015). Fabrication of AgBr nanomaterials as excellent antibacterial agents. *RSC Advances*, *5*(89), 72872–72880. https://doi.org/10.1039/c5ra12575h

Marambio-Jones, C., & Hoek, E. M. V. (2010). A review of the antibacterial effects of silver nanomaterials and potential implications for human health and the environment. *Journal of Nanoparticle Research*, *12*(5), 1531–1551. https://doi.org/10.1007/s11051-010-9900-y

McLean, R. J. C., Cassanto, J. M., Barnes, M. B., & Koo, J. H. (2001). Bacterial biofilm formation under microgravity conditions. *FEMS Microbiology Letters*, *195*(2), 115–119. https://doi.org/10.1016/S0378-1097(00)00549-8

McQuillan, J. S., Groenaga Infante, H., Stokes, E., & Shaw, A. M. (2012). Silver nanoparticle enhanced silver ion stress response in Escherichia coli K12. *Nanotoxicology*, *6*(8), 857–866. https://doi.org/10.3109/17435390.2011.626532

Melaiye, A., & Youngs, W. J. (2005). Silver and its application as an antimicrobial agent. *Expert Opinion on Therapeutic Patents*, *15*(2), 125–130. https://doi.org/10.1517/13543776.15.2.125

Morones, J. R., Elechiguerra, J. L., Camacho, A., Holt, K., Kouri, J. B., Ramírez, J. T., & Yacaman, M. J. (2005). The bactericidal effect of silver nanoparticles. *Nanotechnology*, *16*(10), 2346–2353. https://doi.org/10.1088/0957-4484/16/10/059

Muirhead, D. L., Technology, B., & Technology, J. (2020). *Chemistry of Ionic Silver and Implications for Design of Potable Water Systems*. 1–12.

Nowack, B., Krug, H. F., & Height, M. (2011). Reply to comments on "120 years of nanosilver history: Implications for policy makers." *Environmental Science and Technology*, *45*(17), 7593–7595. https://doi.org/10.1021/es2017895

Peterson, L. J., & Callahan, M. R. (2007). Overview of potable water systems on spacecraft vehicles and applications for the crew exploration vehicle (CEV). *SAE Technical Papers*, *116*, 492–503. https://doi.org/10.4271/2007-01-3259

Rahaman, M. S., Thérien-Aubin, H., Ben-Sasson, M., Ober, C. K., Nielsen, M., & Elimelech, M. (2014). Control of biofouling on reverse osmosis polyamide membranes modified with biocidal nanoparticles and antifouling polymer brushes. *Journal of Materials Chemistry B*, *2*(12), 1724–1732. https://doi.org/10.1039/c3tb21681k

Reinsch, B. C., Levard, C., Li, Z., Ma, R., Wise, A., Gregory, K. B., Brown, G. E., & Lowry, G. V. (2012). Sulfidation of silver nanoparticles decreases Escherichia coli growth inhibition. *Environmental Science and Technology*, *46*(13), 6992–7000. https://doi.org/10.1021/es203732x

Rice, D., Barrios, A. C., Xiao, Z., Bogler, A., Zeev, E. B., & Perreault, F. (2018). Development of anti-biofouling feed spacers to improve performance of reverse osmosis modules. *Water Research*, *145*, 599–607. https://doi.org/10.1016/J.WATRES.2018.08.068

Roberts, M. S., Hummerick, M. E., Edney, S. L., Bisbee, P. A., Callahan, M. R., Loucks, S., Pickering, K. D., & Sager, J. C. (2007). Assessment of silver based disinfection technology for CEV and future US spacecraft: Microbial efficacy. *SAE Technical Papers*, *116*, 481–491. https://doi.org/10.4271/2007-01-3142

Roy, A., Bulut, O., Some, S., Mandal, A. K., & Yilmaz, M. D. (2019). Green synthesis of silver nanoparticles: Biomolecule-nanoparticle organizations targeting antimicrobial

activity. *RSC Advances*, *9*(5), 2673–2702. https://doi.org/10.1039/c8ra08982e

Sambhy, V., MacBride, M. M., Peterson, B. R., & Sen, A. (2006). Silver bromide nanoparticle/polymer composites: Dual action tunable antimicrobial materials. *Journal of the American Chemical Society*, *128*(30), 9798–9808. https://doi.org/10.1021/ja061442z

Silvestry-Rodriguez, N., Bright, K. R., Slack, D. C., Uhlmann, D. R., & Gerba, C. P. (2008). Silver as a residual disinfectant to prevent biofilm formation in water distribution systems. *Applied and Environmental Microbiology*, *74*(5), 1639–1641. https://doi.org/10.1128/AEM.02237-07

Sim, W., Barnard, R. T., Blaskovich, M. A. T., & Ziora, Z. M. (2018). Antimicrobial silver in medicinal and consumer applications: A patent review of the past decade (2007–2017). *Antibiotics*, *7*(4), 1–15. https://doi.org/10.3390/antibiotics7040093

Singh, G., Babele, P. K., Shahi, S. K., Sinha, R. P., Tyagi, M. B., & Kumar, A. (2014). Green synthesis of silver nanoparticles using cell extracts of Anabaena doliolum and screening of its antibacterial and antitumor activity. *Journal of Microbiology and Biotechnology*, *24*(10), 1354–1367. https://doi.org/10.4014/jmb.1405.05003

Suchomel, P., Kvitek, L., Panacek, A., Prucek, R., Hrbac, J., Vecerova, R., & Zboril, R. (2015). Comparative Study of Antimicrobial Activity of AgBr and Ag Nanoparticles (NPs). *PLoS ONE*, *10*(3), 1–15. https://doi.org/10.1371/journal.pone.0119202

Tylkowski, B., Trojanowska, A., Nowak, M., Marciniak, L., & Jastrzab, R. (2019). Applications of silver nanoparticles stabilized and/or immobilized by polymer matrixes. *Physical Sciences Reviews*, *2*(7), 1–16. https://doi.org/10.1515/psr-2017-0024

Vazquez-Muñoz, R., Borrego, B., Juárez-Moreno, K., García-García, M., Mota Morales, J. D., Bogdanchikova, N., & Huerta-Saquero, A. (2017). Toxicity of silver nanoparticles in biological systems: Does the complexity of biological systems matter? *Toxicology Letters*, *276*(December 2016), 11–20. https://doi.org/10.1016/j.toxlet.2017.05.007

Verkhovskii, R., Kozlova, A., Atkin, V., Kamyshinsky, R., Shulgina, T., & Nechaeva, O. (2019). Physical properties and cytotoxicity of silver nanoparticles under different polymeric stabilizers. *Heliyon*, *5*(3), e01305. https://doi.org/10.1016/j.heliyon.2019.e01305

WHO. (2018). Silver as a drinking-water disinfectant. In *Alternative drinking-water disinfectants: bromine, iodine and silver*. http://apps.who.int/bookorders.

Williamson, J. P., & Emmert, G. L. (2013). A flow injection analysis system for monitoring silver (I) ion and iodine residuals in recycled water from recovery

systems used for spaceflight. In *Analytica Chimica Acta* (Vol. 792, pp. 72–78). https://doi.org/10.1016/j.aca.2013.07.011

Wu, S., Altenried, S., Zogg, A., Zuber, F., Maniura-Weber, K., & Ren, Q. (2018). Role of the Surface Nanoscale Roughness of Stainless Steel on Bacterial Adhesion and Microcolony Formation. *ACS Omega*, *3*(6), 6456–6464. https://doi.org/10.1021/acsomega.8b00769

Xiu, Z. M., Zhang, Q. B., Puppala, H. L., Colvin, V. L., & Alvarez, P. J. J. (2012). Negligible particle-specific antibacterial activity of silver nanoparticles. *Nano Letters*, *12*(8), 4271–4275. https://doi.org/10.1021/nl301934w

Yamaguchi, N., Roberts, M., Castro, S., Oubre, C., Makimura, K., Leys, N., Grohmann, E., Sugita, T., Ichijo, T., & Nasu, M. (2014). Microbial monitoring of crewed habitats in space—current status and future perspectives. *Microbes and Environments*, *29*(3), 250–260. https://doi.org/10.1264/jsme2.ME14031

Yang, J., Thornhill, S. G., Barrila, J., Nickerson, C. A., Ott, C. M., & McLean, R. J. C. (2018). Microbiology of the Built Environment in Spacecraft Used for Human Flight. In *Methods in Microbiology* (1st ed., Vol. 45, Issue October). Elsevier Ltd. https://doi.org/10.1016/bs.mim.2018.07.002

Zawadzka, K., Kądzioła, K., Felczak, A., Wrońska, N., Piwoński, I., Kisielewska, A., & Lisowska, K. (2014). Surface area or diameter - Which factor really determines the antibacterial activity of silver nanoparticles grown on TiO2 coatings? *New Journal of Chemistry*, *38*(7), 3275–3281. https://doi.org/10.1039/c4nj00301b

Zea, L., McLean, R. J. C., Rook, T. A., Angle, G., Carter, D. L., Delegard, A., Denvir, A., Gerlach, R., Gorti, S., McIlwaine, D., Nur, M., Peyton, B. M., Stewart, P. S., Sturman, P., & Velez Justiniano, Y. A. (2020). Potential biofilm control strategies for extended spaceflight missions. *Biofilm*, *2*(January), 100026. https://doi.org/10.1016/j.bioflm.2020.100026

APPENDIX A

EDX IMAGES

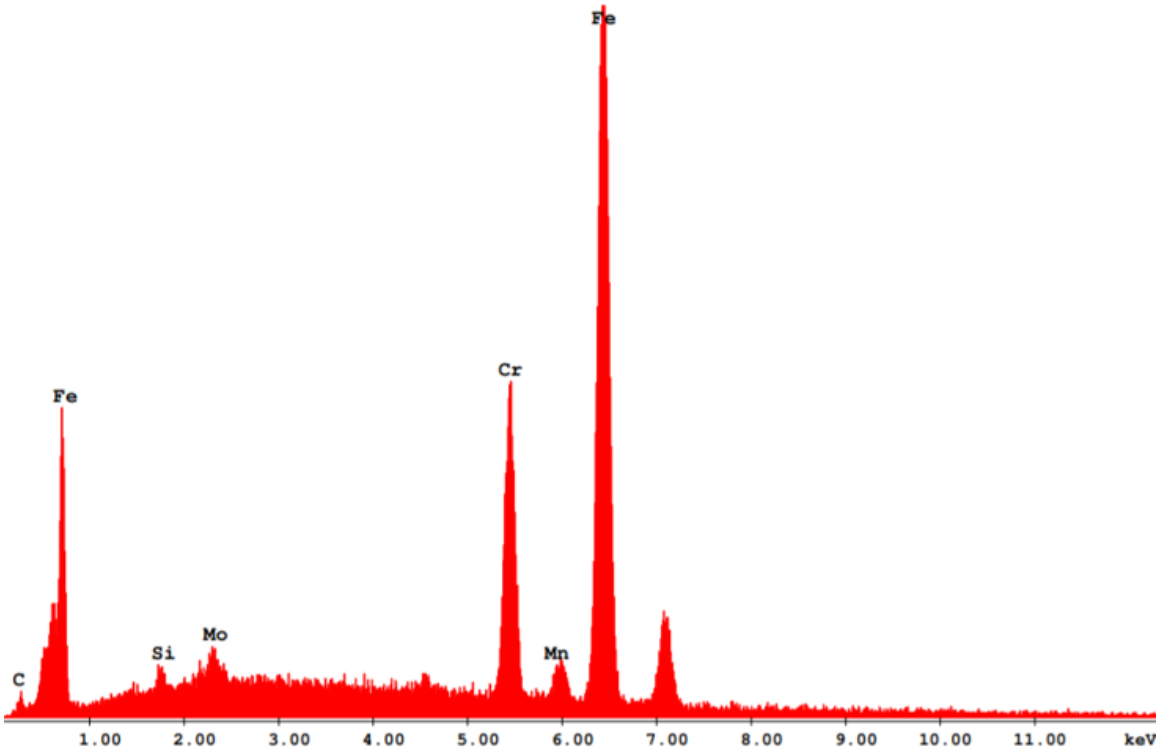

Figure A1: EDX image of pristine stainless steel

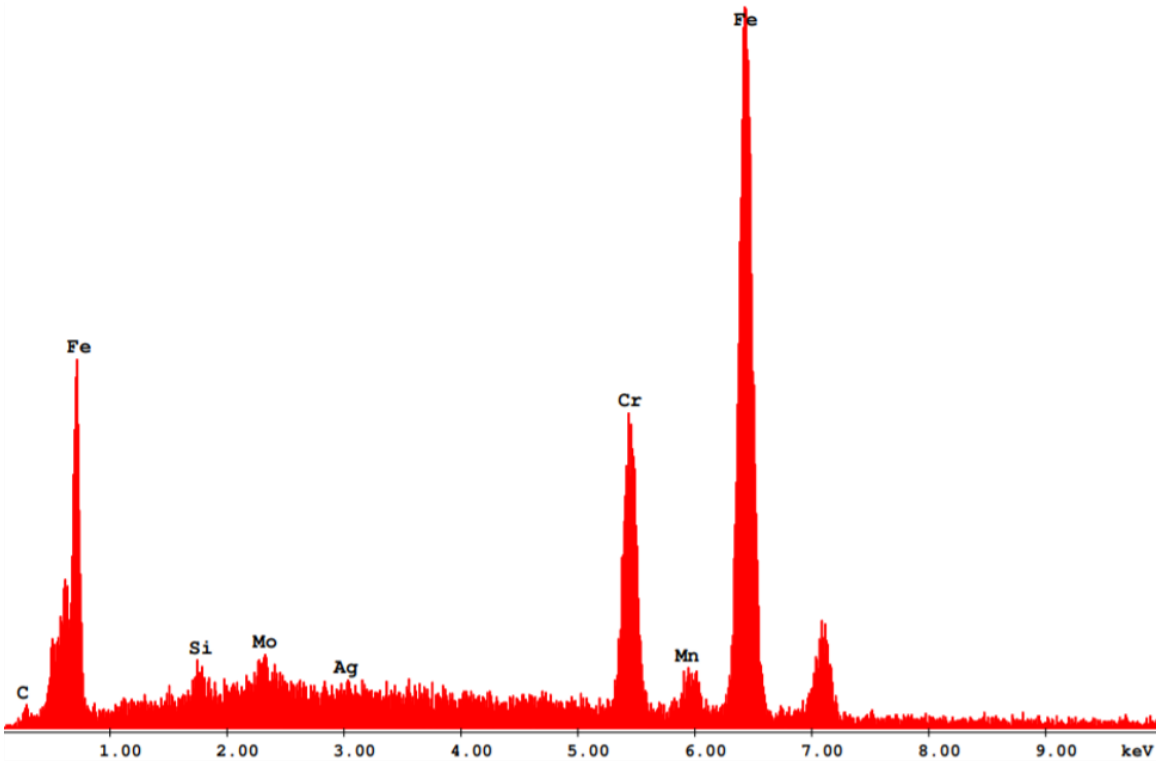

Figure A2: EDX Image of AgNPs-functionalized stainless steel

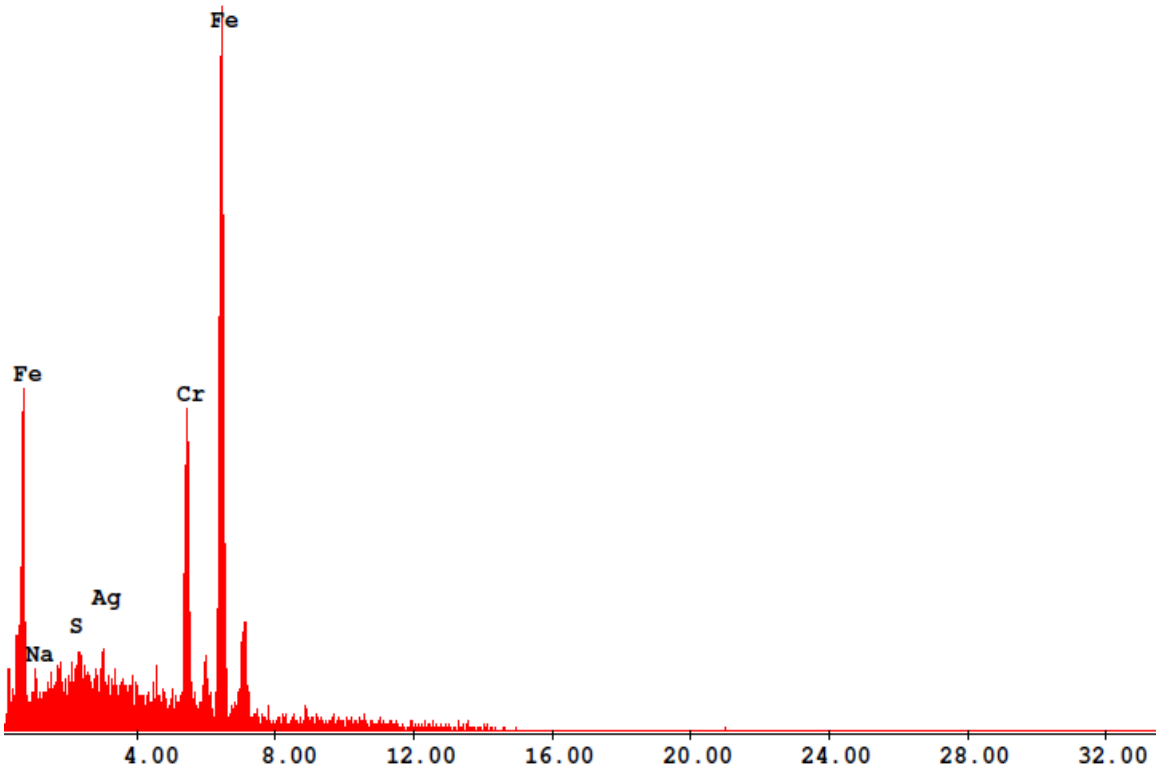

Figure A3: EDX Image of 10 $^{-1}$M Na_2S-functionalized stainless steel

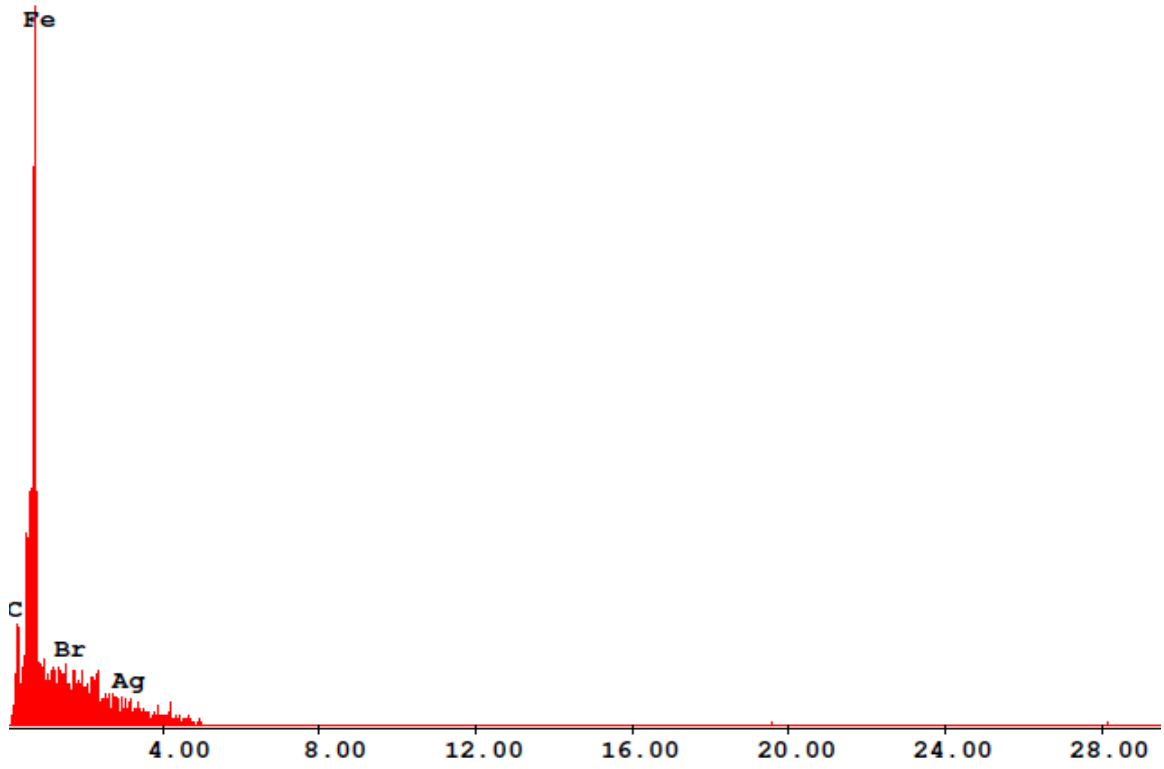

Figure A4: EDX Image of 10 $^{-1}$M NaBr-functionalized stainless steel

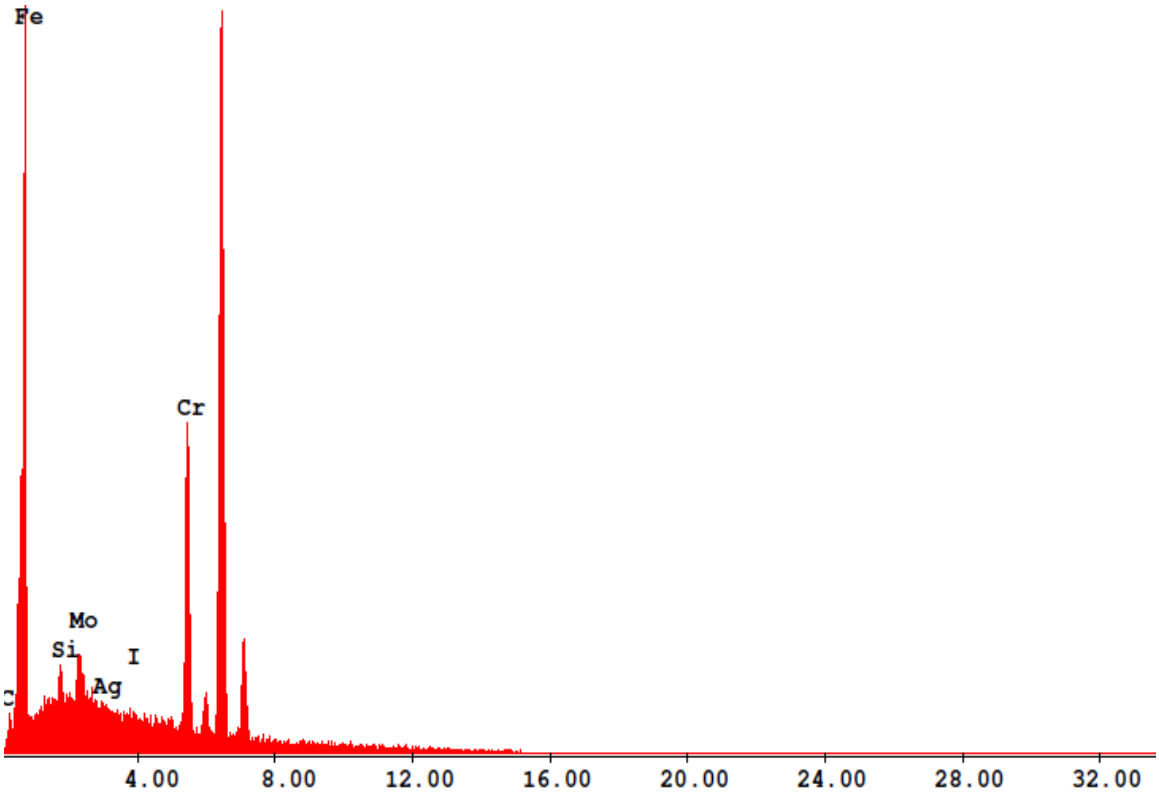

Figure A5: EDX Image of 10 $^{-1}$M NaI-functionalized stainless steel